

SCIENTIFIC REPORTS



OPEN

Improved NO₂ Gas Sensing Properties of Graphene Oxide Reduced by Two-beam-laser Interference

Li Guo¹, Ya-Wei Hao¹, Pei-Long Li¹, Jiang-Feng Song¹, Rui-Zhu Yang¹, Xiu-Yan Fu², Sheng-Yi Xie³, Jing Zhao⁴ & Yong-Lai Zhang²

We report on the fabrication of a NO₂ gas sensor from room-temperature reduction of graphene oxide(GO) via two-beam-laser interference (TBLI). The method of TBLI gives the distribution of periodic dissociation energies for oxygen functional groups, which are capable to reduce the graphene oxide to hierarchical graphene nanostructures, which holds great promise for gaseous molecular adsorption. The fabricated reduced graphene oxide(RGO) sensor enhanced sensing response in NO₂ and accelerated response/recovery rates. It is seen that, for 20 ppm NO₂, the response (R_a/R_g) of the sensor based on RGO hierarchical nanostructures is 1.27, which is higher than that of GO (1.06) and thermal reduced RGO (1.04). The response time and recovery time of the sensor based on laser reduced RGO are 10 s and 7 s, which are much shorter than those of GO (34 s and 45 s), indicating that the sensing performances for NO₂ sensor at room temperature have been enhanced by introduction of nanostructures. This mask-free and large-area approach to the production of hierarchical graphene micro-nanostructures, could lead to the implementation of future graphene-based sensors.

Nitrogen dioxide (NO₂), mainly released by automotive emissions and combustion of conventional fossil fuels, is one of the common air pollutants and can also threaten the health of human beings, because it could bring several serious diseases even at low concentrations. Therefore, the development of high performance gas sensor to detect the gas of NO₂ in an economic way is crucially important, for not only health protection but also environmental applications. Since the ability to detect individual gas molecules by graphene was demonstrated¹, considerable numbers of research activities have been ignited for graphene-based gas sensors²⁻⁷, including flexible gas sensors for wearable sensing applications^{8,9}, and NO₂ detecting sensors¹⁰⁻¹³, because graphene and its derivatives exhibit great electronic conductivity, flexibility, low noise and good thermal stability, it has been generally considered as a promising gas-sensing material for various highly sensitive detections. But interaction between intrinsic graphene and gas molecules is weak, in contrast, the surface of graphene oxide contains a large number of chemically active defects, showing remarkably improvement in adsorption capacity and large-scale preparation¹⁴⁻¹⁸. However, the surface area is reduced due to the sheet stacking, which seriously restricts the development of graphene-based gas sensors. In order to make the interior sheet fully contact to the test gas, it is necessary to prepared micro-nano hierarchical structure on the film to expand the specific surface area of material, and then, to improve the performance of the device. Researchers have developed nanostructured materials such as a 3-dimensional (3D) graphene foam network and a graphene nanomesh to overcome low-level sensitivity and slow response of graphene-based gas sensors¹⁹⁻²³. Han *et al.* reported porous grapheme oxide network for chemical sensing via steam etching²⁰. Yavari *et al.* using the method of CVD fabricated 3-D grapheme foam network for gas detection²¹. Paul *et al.* fabricatied graphene nanomesh using reactive-ion-etching for NO₂ and NH₃ sensing²².

¹Institute of Materials, China Academy of Engineering Physics, Mianyang, Sichuan, 621900, People's Republic of China. ²State Key Laboratory on Integrated Optoelectronics, College of Electronic Science and Engineering, Jilin University 2699 Qianjin Street, Changchun, 130012, People's Republic of China. ³Center for High Pressure Science and Technology Advanced Research, Changchun, 130012, People's Republic of China. ⁴College of Electrical and Electronic Engineering, Changchun University of Technology, Changchun, 130012, People's Republic of China. Correspondence and requests for materials should be addressed to Y.-W.H. (email: haoyawei@caep.cn) or Y.-L.Z. (email: yonglaizhang@jlu.edu.cn)

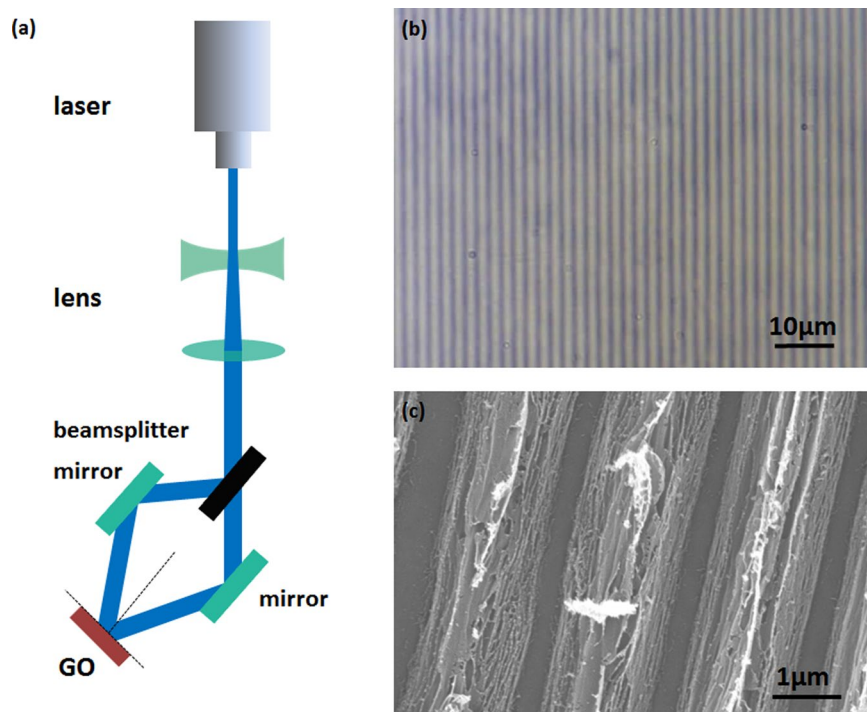


Figure 1. (a) Fabrication scheme of reduction of GO film by two beam laser interference. (b) Optical microscope image of RGO film. (c) SEM image of the grating structure of the graphene surface fabricated at 0.15 W.

Yun *et al.* presented 3D nanostructured RGO scaffold using method of electrostatic self-assembly²³. The method of freeze drying was also reported for the fabricating of 3D graphene/SnO₂ structure²⁴ and 3D SnO₂/RGO structure²⁵. Lupan *et al.* reported a low-powered sensor based on a microtube network²⁶. These methods are limited by restricted temperature, mask, requirement of special equipment and substrate transfer or difficulty in mass production. Here we propose a strategy on the regulation of surface characteristics of graphene oxide using laser micro-nanofabrication technology, to build a high specific surface area of micro-nanostructures and fabricate graphene-based NO₂ sensor. Because GO has good solution process compatibility, the device can be implemented on any substrate, this method does not require a substrate transfer process. Laser micro-nanofabrication can be carried out in the air at room temperature, and it has the advantage of rapid preparation of large areas. By Two-beam-laser Interference method, surface area of the film is increased, the sensitivity of the device towards NO₂ has been enhanced, meanwhile, the response and recovery time is reduced to varying degrees.

Results and Discussion

In this work, TBLI was adopted for larger-area reduction and patterning of GO film towards a RGO gas sensing device. As shown in Fig. 1a, a laser beam of 355 nm wavelength was split into two branches and guided to interfere directly on the surface of a GO film. After 10 seconds of laser exposure, interference occurs. Since distribution of the laser intensity is sinusoidal^{12,27}, the GO film was proposed to be reduced with a similar distribution. Figure 1b shows optical microscopy images of GO film, The periodic patterns could be clearly identified due to the difference in transparencies. SEM images of GO film was shown in Fig. 1c, GO film was patterned into hierarchical nanostructures. This layered nanostructure may result from periodic reduction and ablation of layered graphene oxide stack. The ultrafast removal of interlayer water and oxygen-containing gaseous species occurred during nanosecond laser irradiation. This layered nanostructure hold great promise for guest molecules adsorption and desorption.

C1s XPS was used to measure the surface oxygen contents. As shown in Fig. 2a, the three peaks at 284.6, 286.6 and 288.5 eV are attributed to C-C (nonoxygenated ring carbon), C-O (hydroxyl and epoxy carbon), and C=O (carbonyl), respectively. Notably, the contents of oxygen atoms in pristine GO is as high as 34.8%, the carbon not bonded to oxygen is 65%. After reduction, C-C percentage increases to 76%, indicating the successful removal of oxygen groups.

Raman spectra of pristine GO and RGO films were measured to evaluate the structural change before and after nanosecond laser reduction. As shown in Fig. 2b the I_D/I_G ratios of GO and RGO were 1.07 and 0.99, respectively. A decrease of the I_D/I_G ratio is perhaps an indication of graphitization.

To compare the sensing performance of GO and RGO hierarchical nanostructures, NO₂ sensors were fabricated on ceramic substrates with interdigital electrodes with the laser power of 0.15 W, shown in Figure S1(a). Figure S1(b) presents the current–voltage characteristics of the sensor structure based on GO and RGO. The structure shows a linear behavior for both negative and positive bias voltages in between the −2 V to +2 V region,

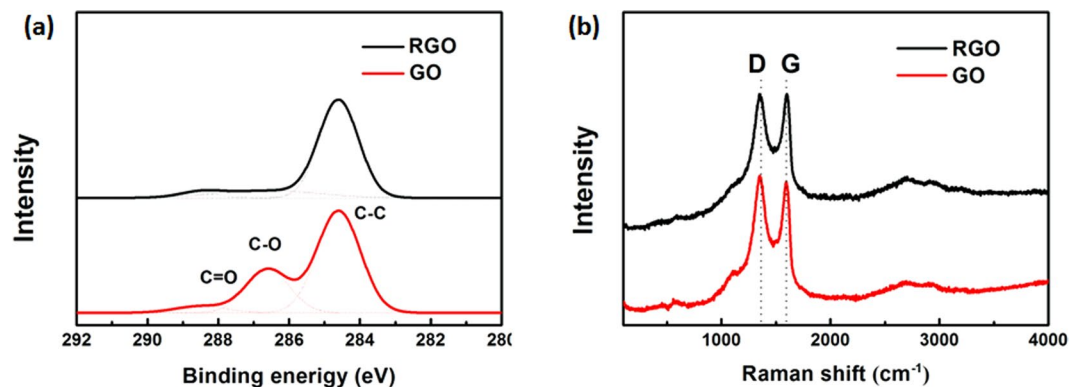


Figure 2. (a) C1s XPS and (b) Raman spectra of pristine GO and RGO.

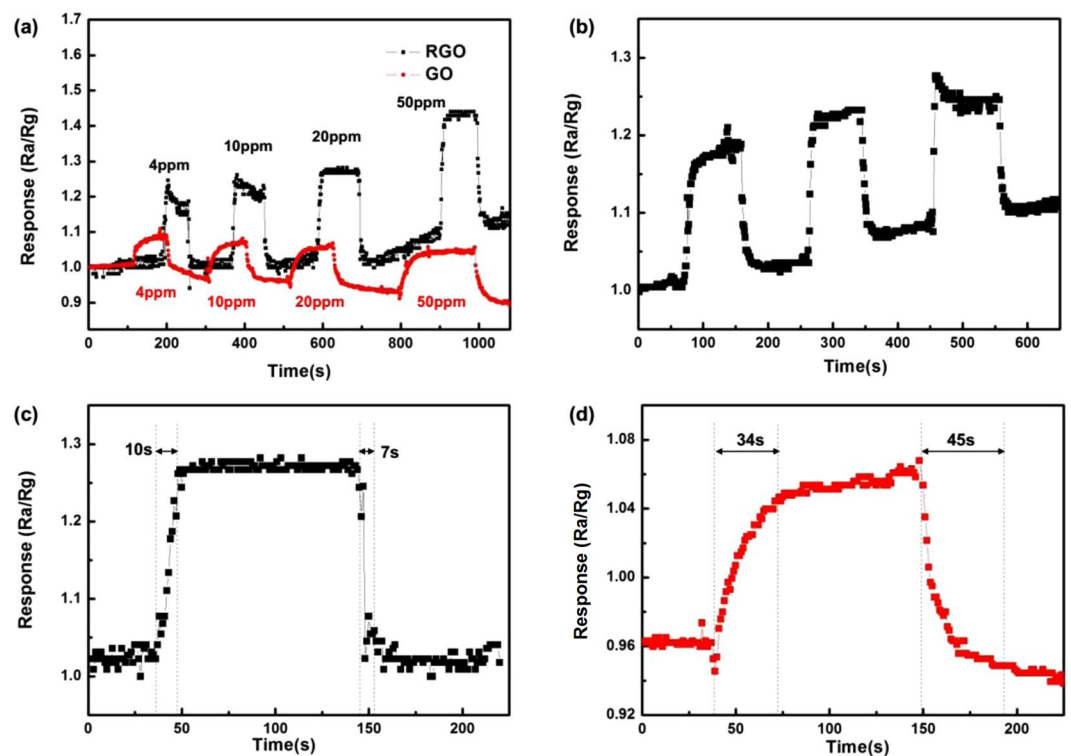


Figure 3. (a) Response and recovery curves of the sensor based on RGO and GO to various NO_2 concentrations at room temperature. (b) The reproducibility of temporal response of RGO exposed to 4ppm NO_2 at room temperature. (c) and (d) The response recovery curves to 20ppm NO_2 of the sensor based on RGO and GO at room temperature, respectively.

and indicates the formation of ohmic contacts between the electrode and GO(RGO). However, at higher applied bias voltages an increase in current (decrease in resistance) can be observed. This effect can be related to the self-heating effect of the aerographite-based sensing material, as was already observed for other carbon based structures²⁶. After laser reduction, the electrical resistance of the device decreased from 50.2 to 11.7 k Ω .

Figure 3a shows the response and recovery curves to 4–50 ppm NO_2 of the sensors at room temperature. It is seen that the response of the sensor based on RGO is larger than that of GO, indicating the enhancing sensing response by introduction of hierarchical nanostructures (The binding energy of GO and NO_2 molecule is stronger than that of RGO, according to our calculations). The variety of response range is caused by two factors together, the increased specific surface area and the reduced oxygen containing groups. We can speculate that in the case of functional groups are invariant, the hierarchical nanostructures would improve the sensitivity of the device to a greater extent. As shown in Fig. 3b, the response variability range is almost constant for 3 cycles to 4ppm NO_2 , indicating the reliability of our RGO NO_2 sensor. Figure 3c,d shows the response and recovery curves to 20ppm NO_2 of the sensor based on GO and RGO hierarchical nanostructures at room temperature. The resistances of the devices were decreased upon exposure to NO_2 gas, indicating NO_2 doped the RGO film with holes, as RGO film

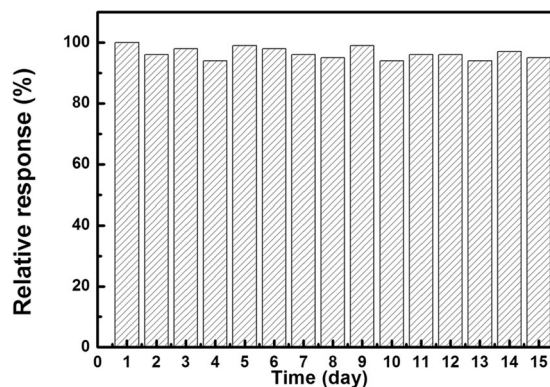


Figure 4. The long-time stability of RGO sensor for NO₂ sensing.

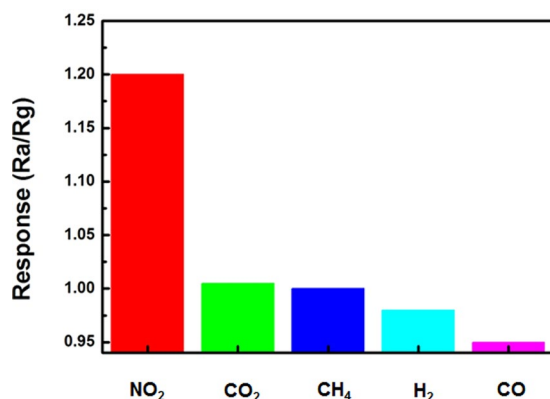


Figure 5. Detection selectivity of RGO sensor upon exposure to various vapors (~4 ppm) operating at room temperature.

exhibited the electrical behavior of a p-type semiconductor^{1,28}. It is seen that the response of the sensor based on RGO hierarchical nanostructures is 1.27, which is higher than that of GO (1.06), indicating the enhanced sensing response by laser reduction of GO nanostructures. The response time and recovery time of the sensor based on nanostructured RGO are 10 s and 7 s, respectively, which are much shorter than that of GO (34 s and 45 s). Figure 4. shows response of the RGO sensor to 4 ppm NO₂ for 15 days. It is seen that the response of the sensor floats slightly. The observed results reveal that RGO sensor exhibits good stability. The selectivity of the RGO sensor towards NO₂ is also examined, as shown in Fig. 5. It is seen that the response of the sensor to 4 ppm NO₂ is 1.2, which is much larger than those of the sensor to 4 ppm other gases, such as CO₂, CH₄, H₂ and CO, indicating that the NO₂ sensor exhibits good selectivity and can be used for selective detection of NO₂. The sensing performances of the sensor were also compared with the previously reported sensors based on micro-nano structured graphene materials, as shown in Table 1.

As a comparison, RGO film reduced at 300 °C under the protection of nitrogen has similar oxygen content with that of RGO reduced by laser interference (shown in Figure S2). When expose thermal reduced RGO to 20 ppm NO₂, the value of R_a/R_g is 1.04, lower than that of reduced RGO by laser, which confirms the importance of nanostructures in the NO₂ sensor. Based on the above results, the fabricated RGO sensor shows improved sensing response in NO₂ and accelerated response/recovery rates. We also tested the response of gas sensors based on GO and RGO ethanol gas (Figure S3). Different from NO₂, the resistances of the devices were increased upon exposure to ethanol gas, indicating ethanol doped the RGO film with electrons. As shown in Figure S4, binding energy of single layer graphene oxide decreased severely due to the shrinking of oxygen containing groups, sensitivity of RGO hierarchical nanostructures is lower than GO. The response and recovery times of the device fabricated by laser are improved obviously. Once again we confirmed that the hierarchical nanostructures could improve the response and recovery times of the device.

To get further insight into the different mechanisms of the gas sensors, first principle study was carried out to give an essential explanation (Figure 6 and S4). In the present calculations. The binding energy between NO₂ molecule and graphene is 78 meV, which is smaller than the interaction of NO₂ and hydroxyl groups of graphene oxide. For epoxy group, a negative binding energy of -144 meV indicating a coulomb repulsion between epoxy and NO₂ will push the molecules away from the GO sheet. Overall, according to other studies²⁹, the oxygen functional groups on GO would hold significantly larger ability to absorb NO₂ molecules than pure graphene. In this work, the RGO film shows a stronger response than GO film under the influence of the formation of nanostructure and the reduction of oxygen-containing functional groups. However, as shown in Figure S3, for ethanol,

properties of sensing material	Preparation method	Tested gas (ppm)	Gas response	Operating temperature(°C)	Response time(τ_r /s)	Recovery time (τ_d /s)	Year of publication	Ref.
Aerographite	Chemical vapour deposition	CO ₂ (500) NH ₃ (100) H ₂ (10000)	3.83% 1.21% 31.84% ($\Delta R/R_0$)	RT RT RT	3.98 8.7 0.25	6.92 11.58 0.35	2016	26
3D graphene foam network	Chemical vapour deposition	NH ₃ (1000)	30% ($\Delta R/R_0$)	RT	~500	~800	2011	21
3D graphene/SnO ₂	Freeze drying	NO ₂ (50)	6% ($\Delta R/R_0$)	RT	190	224	2014	24
3D SnO ₂ /RGO	Freeze drying	NO ₂ (100)	1.079 (R_u/R_g)	55	>310 ^a	373	2015	25
Graphene nanomesh	Nanosphere lithography	NO ₂ (10)	11% ^a ($\Delta R/R_0$)	RT	>300 ^a	>300 ^a	2012	22
RGO nanofibers	Electrostatic self-assembly	NO ₂ (4.5)	20% ($\Delta R/R_0$)	RT	>300 ^a	>300 ^a	2014	23
Porous Graphene Oxide Network	Steam Etched	NO ₂ (250)	8% ($\Delta R/R_0$)	RT	~200 ^a	~400 ^a	2011	20
This work	Two-beam-laser Interference	NO ₂ (4) NO ₂ (20)	1.2 1.27 (R_u/R_g)	RT	<10 10	<10 7		

Table 1. Comparison of sensing performances of our NO₂ sensor with other published gas sensors based on micro-nano structured graphene-based materials. ^aEstimated from graphical plot.

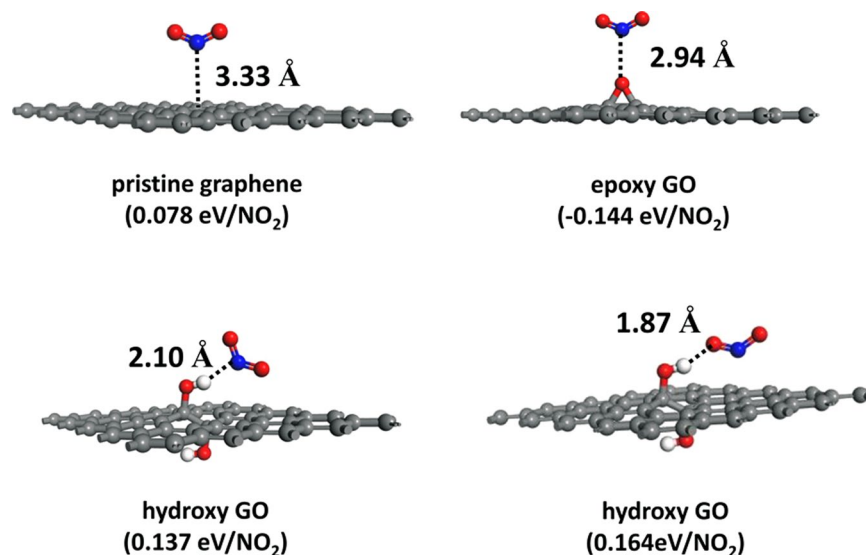


Figure 6. First-principle study of the interaction between NO₂ molecule and graphene sheets, as well as epoxy or hydroxyl groups functionalized graphene.

binding energy between a gas molecule and hydroxyl groups of graphene oxide is larger than the interaction of ethanol and graphene obviously, for the hydrogen bond between the oxygen group and hydroxyl of ethanol will decrease the energy.

Conclusion

A graphene-based NO₂ sensor has been successfully fabricated by TBLI reduction and nanostructuring of GO film. The presence of nanostructure increases the surface area and thus significantly improves the sensitivity of the device towards NO₂, meanwhile, the response and recovery time is reduced to varying degrees at room temperature, compared to GO and thermal reduced RGO, this method was proved to be a novel approach to simultaneous reduction and nanostructuring of GO in a surfactant-free, mask-free and large-area manner. Our present study shows great potential for fabrication of high-performance room temperature graphene gas sensors.

Methods

GO was produced via the Hummers method from natural graphite (Aldrich, <150 μm). The GO films were prepared by spin-coating GO solution on ceramic substrates with interdigital electrodes, at 1000 rpm for 30 s, dried at room temperature. The contacts are interdigital Ag-Pd electrodes as shown in the Figure S1(a). The minimum distance between contacts is about 0.2 mm. Then the sample was exposed by two beams which were split from

the UV laser to reduce and produce nanostructures. A frequency-tripled, Q-switched, single-mode Nd:YAG laser (Spectra-physics) with about 10 ns pulse width was used for laser interference. 0.15 W laser power measured before the spectroscopy. The exposure time was 10 s.

The dilute tested gas was air. Gas sensing properties were measured using a static test system. Saturated target vapor was injected into a test chamber (about 1 L in volume) by a microinjector through a rubber plug. After fully mixed with air (relative humidity was about 25%), the sensor was put into the test chamber. When the response reached a constant value, the sensor was taken out to recover in air. The electrical properties of the sensor were measured by CGS-8 intelligent test meter (Beijing Elite Tech. Co., Ltd, China) <250 mA. The response of a sensor was defined as the ratio (response: $S = R_a/R_g$) of the sensor resistance in air (R_a) to that in the NO₂ (or ethanol) gas (R_g). The time taken by the sensor to achieve 90% of the total resistance change was defined as the response time in the case of adsorption and recovery time in the case of desorption. X-ray photoelectron spectroscopy (XPS) was performed using an ESCALAB 250 spectrometer. Scanning electron microscope (SEM) experiments were performed on a Hitachi S-4800 electron microscope. Optical microscope images were obtained from a Motic BE400 microscope. Raman spectra were measured with a Renishaw Raman microscope using 514 nm wavelength laser.

First principles calculations are based on generalized gradient approximation of Perdew-Burke-Ernzerhof implemented in VASP code. Projector augmented wave method is used to describe the electron-ion interaction. The periodic graphene supercell (containing 50 carbon atoms) decorated with oxygen group is used to simulate the graphene oxide. In order to avoid the interaction with neighboring images, a vacuum layer of 20 Å is used. Cutoff energy with 500 eV for plane wave expansion and $2 \times 2 \times 1$ Monkhorst-Pack mesh grid for Brillouin zone sampling are carried out for the calculations.

References

- Schedin, F. *et al.* Detection of individual gas molecules adsorbed on graphene. *Nat. Mater.* **6**, 652–655 (2007).
- Ko, G. *et al.* Graphene-based nitrogen dioxide gas sensors. *Curr. Appl. Phys.* **10**, 1002–1004 (2010).
- Arsat, R. *et al.* Graphene-like nano-sheets for surface acoustic wave gas sensor applications. *Chem. Phys. Lett.* **467**, 344–347 (2009).
- Jung, I. *et al.* Effect of Water Vapor on Electrical Properties of Individual Reduced Graphene Oxide Sheets. *J. Phys. Chem. C* **112**, 20264–20268 (2008).
- Hwang, E. H., Adam, S. & Das Sarma, S. Transport in chemically doped graphene in the presence of adsorbed molecules. *Phys. Rev. B* **76** (2007).
- Antonova, I. V. *et al.* Extremely high response of electrostatically exfoliated few layer graphene to ammonia adsorption. *Nanotechnology* **22** (2011).
- Ratinac, K. R., Yang, W. R., Ringer, S. P. & Braet, F. Toward Ubiquitous Environmental Gas Sensors-Capitalizing on the Promise of Graphene. *Environ. Sci. Technol.* **44**, 1167–1176 (2010).
- Duy, L. T. *et al.* Flexible Transparent Reduced Graphene Oxide Sensor Coupled with Organic Dye Molecules for Rapid Dual-Mode Ammonia Gas Detection. *Adv. Funct. Mater.* **26**, 4329–4338 (2016).
- Choi, H. *et al.* Flexible and Transparent Gas Molecule Sensor Integrated with Sensing and Heating Graphene Layers. *Small* **10**, 3685–3691 (2014).
- Long, H. *et al.* High Surface Area MoS₂/Graphene Hybrid Aerogel for Ultrasensitive NO₂ Detection. *Adv. Funct. Mater.* **26**, 5158–5165 (2016).
- Bai, S. L. *et al.* Enhancement of NO₂-Sensing Performance at Room Temperature by Graphene-Modified Polythiophene. *Ind. Eng. Chem. Res.* **55**, 5788–5794 (2016).
- Ridene, M., Iezhokin, I., Offermans, P. & Flipse, C. F. J. Enhanced Sensitivity of Epitaxial Graphene to NO₂ by Water Coadsorption. *J. Phys. Chem. C* **120**, 19107–19112 (2016).
- Wu, J. *et al.* Chemically functionalized 3D graphene hydrogel for high performance gas sensing. *J. Mater. Chem. A* **4**, 8130–8140 (2016).
- Lu, G. H. *et al.* Toward Practical Gas Sensing with Highly Reduced Graphene Oxide: A New Signal Processing Method to Circumvent Run-to-Run and Device-to-Device Variations. *ACS Nano* **5**, 1154–1164 (2011).
- Li, W. W. *et al.* Reduced Graphene Oxide Electrically Contacted Graphene Sensor for Highly Sensitive Nitric Oxide Detection. *ACS Nano* **5**, 6955–6961 (2011).
- Fowler, J. D. *et al.* Practical Chemical Sensors from Chemically Derived Graphene. *ACS Nano* **3**, 301–306 (2009).
- Paul, R. K., Badhulika, S., Saucedo, N. M. & Mulchandani, A. Graphene Nanomesh As Highly Sensitive Chemiresistor Gas Sensor. *Anal. Chem.* **84**, 8171–8178 (2012).
- Dua, V. *et al.* All-organic vapor sensor using inkjet-printed reduced graphene oxide. *Angew. Chem. Int. Ed.* **49**, 2154–2157 (2010).
- Chen, Z. *et al.* Three-Dimensional Crumpled Graphene-Based Nanosheets with Ultrahigh NO₂ Gas Sensibility. *ACS Appl. Mater. Interfaces* **9**, 11819–11827 (2017).
- Han, T. H., Huang, Y. K., Tan, A. T. L., Dravid, V. P. & Huang, J. X. Steam Etched Porous Graphene Oxide Network for Chemical Sensing. *JACS* **133**, 15264–15267 (2011).
- Yavari, F. *et al.* High Sensitivity Gas Detection Using a Macroscopic Three-Dimensional Graphene Foam Network. *Scientific Reports* **1**, 5 (2011).
- Paul, R. K., Badhulika, S., Saucedo, N. M. & Mulchandani, A. Graphene nanomesh as highly sensitive chemiresistor gas sensor. *Anal. Chem.* **84**, 8171–8178 (2012).
- Yun, Y. J. *et al.* A 3D scaffold for ultra-sensitive reduced graphene oxide gas sensors. *Nanoscale* **6**, 6511–6514 (2014).
- Liu, X., Cui, J., Sun, J. & Zhang, X. 3D graphene aerogel-supported SnO₂ nanoparticles for efficient detection of NO₂. *RSC Adv.* **4**, 22601–22605 (2014).
- Li, L., He, S., Liu, M., Zhang, C. & Chen, W. Three-Dimensional Mesoporous Graphene Aerogel-Supported SnO₂ Nanocrystals for High-Performance NO₂ Gas Sensing at Low Temperature. *Anal. Chem.* **87**, 1638–1645 (2015).
- Lupan, O. *et al.* Low powered, tunable and ultra-light aerographite sensor for climate relevant gas monitoring. *J. Mater. Chem. A* **4**, 16723–16730 (2016).
- Guo, L. *et al.* Two-beam-laser interference mediated reduction, patterning and nanostructuring of graphene oxide for the production of a flexible humidity sensing device. *Carbon* **50**, 1667–1673 (2012).
- Leenaerts, O., Partoens, B. & Peeters, F. M. Adsorption of H₂O, NH₃, CO, NO₂, and NO on graphene: A first-principles study. *Phys. Rev. B* **77**, 6 (2008).
- Tang, S. B. & Cao, Z. X. Adsorption of nitrogen oxides on graphene and graphene oxides: Insights from density functional calculations. *J. Chem. Phys.* **134**, 14 (2011).

Acknowledgements

The authors gratefully acknowledge financial support from the NSFC (Grant Nos. 61405015 and 61603059).

Author Contributions

L.G., Y.W.H. and Y.L.Z. conceived the study; L.G., P.L.L., Y.Y.F., J.Z. and S.Y. X. did most of the experiments; L.G., Y.W.H., R.Z.Y., J.F.S., S.Y.X. and Y.L.Z. analyzed the data and wrote the manuscript.

Additional Information

Supplementary information accompanies this paper at <https://doi.org/10.1038/s41598-018-23091-1>.

Competing Interests: The authors declare no competing interests.

Publisher's note: Springer Nature remains neutral with regard to jurisdictional claims in published maps and institutional affiliations.



Open Access This article is licensed under a Creative Commons Attribution 4.0 International License, which permits use, sharing, adaptation, distribution and reproduction in any medium or format, as long as you give appropriate credit to the original author(s) and the source, provide a link to the Creative Commons license, and indicate if changes were made. The images or other third party material in this article are included in the article's Creative Commons license, unless indicated otherwise in a credit line to the material. If material is not included in the article's Creative Commons license and your intended use is not permitted by statutory regulation or exceeds the permitted use, you will need to obtain permission directly from the copyright holder. To view a copy of this license, visit <http://creativecommons.org/licenses/by/4.0/>.

© The Author(s) 2018